THE JOURNAL OF BIOLOGICAL CHEMISTRY VOL. 289, NO. 27, pp. 19089–19097, July 4, 2014

YfgM Is an Ancillary Subunit of the SecYEG Translocon in *Escherichia coli*[*]

Received for publication, December 12, 2013, and in revised form, March 19, 2014 Published, JBC Papers in Press, May 22, 2014, DOI 10.1074/jbc.M113.541672

Hansjörg Götzke[‡], Isolde Palombo[‡], Claudio Muheim[‡], Elsa Perrody[§], Pierre Genevaux[§], Renuka Kudva[¶‖], Matthias Müller[¶‖], and Daniel O. Daley[‡1]

From the [‡]Center for Biomembrane Research, Department of Biochemistry and Biophysics, Stockholm University, SE-106 91 Stockholm, Sweden, [§]Laboratoire de Microbiologie et Génétique Moléculaires, CNRS, and Université Paul Sabatier, 31062 Toulouse, France, and [¶]Institute of Biochemistry and Molecular Biology, Zentrum für Biochemie und Molekulare, [‖]Spemann Graduate School of Biology and Medicine, University of Freiburg, D-79104 Freiburg, Germany

Background: The Sec translocon mediates protein secretion in all organisms.
Results: YfgM interacts with the Sec translocon and is part of a periplasmic chaperone network in *Escherichia coli.*
Conclusion: We propose that YfgM mediates protein transfer from the Sec translocon to periplasmic chaperones.
Significance: This study provides a better understanding of the composition of the Sec translocon.

Protein secretion in Gram-negative bacteria is essential for both cell viability and pathogenesis. The vast majority of secreted proteins exit the cytoplasm through a transmembrane conduit called the Sec translocon in a process that is facilitated by ancillary modules, such as SecA, SecDF-YajC, YidC, and PpiD. In this study we have characterized YfgM, a protein with no annotated function. We found it to be a novel ancillary subunit of the Sec translocon as it co-purifies with both PpiD and the SecYEG translocon after immunoprecipitation and blue native/SDS-PAGE. Phenotypic analyses of strains lacking *yfgM* suggest that its physiological role in the cell overlaps with the periplasmic chaperones SurA and Skp. We, therefore, propose a role for YfgM in mediating the trafficking of proteins from the Sec translocon to the periplasmic chaperone network that contains SurA, Skp, DegP, PpiD, and FkpA.

A number of different protein secretion systems are available in Gram-negative bacteria; however, the vast majority of secreted proteins utilize a transmembrane conduit called the Sec translocon (SecYEG in *Escherichia coli*) (1, 2). This multipurpose device can facilitate co-translational insertion of proteins into the inner membrane and post-translational translocation of proteins to the periplasmic space (3–6). The latter category includes lipoproteins, β-barrel proteins, and extracellular proteins, which are subsequently trafficked from the periplasm to their final destination by other dedicated pathways (7–11).

There is considerable interest in understanding how the Sec translocon inserts and translocates proteins. Crystal structures indicate that it has an hourglass shape with a central constriction that comprises a ring of hydrophobic residues and a short "plug" helix (12–15). An opening between transmembrane helices 2 and 7 is postulated to act as a lateral-exit gate for signal sequences and transmembrane helices. Current opinion favors a model whereby docking of a signal sequence or a transmembrane helix at the lateral-exit gate signals movement of the plug and enables protein translocation (3–6).

The Sec translocon is essentially a passive pore, and it requires ancillary modules to facilitate insertion and/or translocation. For example, translational elongation by the ribosome provides a driving force for co-translational insertion of inner membrane proteins (3–6), and YidC facilitates their insertion into the lipid bilayer (16–18). Secreted proteins and large soluble domains in membrane proteins are "pushed" through the translocon by SecA and the SecDF-YajC complex (15, 19, 20). The ancillary modules can in most cases be co-purified with the translocon after detergent solubilization (17, 18, 21, 22); thus, it seems likely that they are physically associated in the lipid bilayer.

Have all ancillary modules of the Sec translocon been identified? Recently we reported that YfgM, a protein with no annotated function, interacts with PpiD in the inner membrane of *E. coli* (23). Because PpiD is thought to act as a periplasmic gatekeeper for the translocon (24), we reasoned that YfgM might have a similar role. YfgM (like PpiD) is an inner membrane protein with a single transmembrane helix and a large C-terminal periplasmic domain (23, 25, 26). In this study we present data that indicate that YfgM interacts with the SecYEG translocon and that it operates in the periplasmic chaperone network consisting of SurA, Skp, DegP, PpiD, and FkpA.

EXPERIMENTAL PROCEDURES

Bacterial Strains and Microbial Techniques—All strains and plasmids used in this study are listed in Table 1. Plasmids were constructed using standard molecular biology techniques or the In-Fusion HD Cloning kit (Clontech). Site-directed mutagenesis was performed using the QuikChange Site-directed Mutagenesis kit (Stratagene). All plasmids were confirmed by sequencing (MWG). Disruption of chromosomal genes in MC4100 and W3110 was carried out by bacteriophage P1 transduction from the Keio collection (27). In some strains

* This work was supported by a grant from the Swedish Research Council (to D. O. D.).
[1] To whom correspondence should be addressed: Center for Biomembrane Research, Dept. of Biochemistry and Biophysics, Stockholm University, Svante Arrhenius väg 16c, SE-106 91 Stockholm, Sweden. Tel.: 46-8-16-29-10; Fax: 46-8-15-36-79; E-mail: ddaley@dbb.su.se.

TABLE 1
Bacterial strains and plasmids

	Relevant characteristics	Reference or source
Strains		
BL21(DE3)	Carrying *pLysS*	Invitrogen
W3110		Our collection
Δ*yfgM* Δ*ppiD*	W3110 Δ*yfgM* + *ppiD*::*kan*	This study
MC4100		Our collection
Δ*degP*	MC4100 *degP*::*kan*	M. Sousa
Δ*yfgM*	MC4100 *yfgM*::*kan*	This study
Δ*skp*	MC4100 *skp*::*kan*	This study
Δ*surA*	MC4100 *surA*::*kan*	This study
Δ*ppiD*	MC4100 *ppiD*::*kan*	This study
Δ*yfgM* Δ*ppiD*	MC4100 Δ*ppiD* + *yfgM*::*kan*	This study
Δ*yfgM* Δ*degP*	MC4100 Δ*degP* + *yfgM*::*kan*	This study
Δ*yfgM* Δ*skp*	MC4100 Δ*skp* + *yfgM*::*kan*	This study
Δ*yfgM* Δ*surA*	MC4100 Δ*surA* + *yfgM*::*kan*	This study
Δ*ppiD* Δ*degP*	MC4100 Δ*degP* + *ppiD*::*kan*	This study
Δ*ppiD* Δ*skp*	MC4100 Δ*ppiD* + *skp*::*kan*	This study
Δ*ppiD* Δ*surA*	MC4100 Δ*ppiD* + *surA*::*kan*	This study
Plasmids		
pSc-*yfgM*	*yfgM* + native promoter in pUA66	This study
pUA66	Low copy plasmid with sc101 origin of replication	(30)
pUA66-*rpoE-gfpmut2* cm	Cm resistance *rpoE rseABC* reporter	This study
pUA66-*ppiA-gfpmut2* cm	Cm resistance *ppiA* reporter	This study
pUA66-*rpoE-gfpmut2*	K_m resistance *rpoE rseABC* reporter	(30)
pUA66-*ppiA-gfpmut2*	K_m resistance *ppiA* reporter	(30)
pCP20	Flp recombinase gene	(28)
pETDuet-*ppiD37H8*	Expression of $PpiD^{SOL}$	This study
pET28a*yfgM45H8*	Expression of $YfgM^{SOL}$	This study

the kanamycin cassette in the target strain was eliminated by the pCP20 method as described in Datsenko and Wanner (28). These strains were confirmed by diagnostic PCR. All strains in this study were cultured at 37 °C in standard LB broth (Difco) supplemented with 25/50 μg/ml kanamycin, 17 μg/ml chloramphenicol, or 50/100 μg/ml ampicillin when necessary.

Immunoprecipitations—Whole cells were grown in 10 ml of M9 minimal media supplemented with 100 μg/ml thiamine, 0.2 (w/v) % glucose, 1 mM $MgSO_4$, 50 μM $CaCl_2$, and 2 mg/ml Complete Supplement Mixture amino acids minus methionine. At an A_{600} of 0.6 the cells were labeled with 15 μCi/ml [^{35}S]methionine for 10 min, then harvested by centrifugation at 5000 × *g* for 10 min. The cell pellet was frozen then thawed on ice and resuspended in 1 ml of immunoprecipitation (IP)[2] buffer (10 mM Tris, pH 8.0, 150 mM NaCl, 20% (w/v) glycerol, Complete Protease Inhibitor Mixture Tablets (Roche Applied Science)). Cell lysis was induced by the addition of 10 mM EDTA, 1 mg/ml lysozyme and incubation on ice for 30 min. 1% (w/v) digitonin (native IPs) or 1% (w/v) Triton X-100, 0.2% (w/v) SDS (denaturing IPs) was added, and lysis was allowed to continue on ice for an additional hour (with occasional vortexing). The extract was retrieved by centrifugation at 21,000 × *g* for 20 min. The preparation yielded enough material for 5 IPs.

The antisera (2.5 μl) were coupled to 10 μl of GammaBind G-Sepharose beads (GE Healthcare) then prewashed with 300 μl of IP buffer. 200 μl of extract was bound by incubation at 4 °C for 30 min and washed 3 times with 300 μl of IP buffer containing either 1% (w/v) digitonin (native IPs) or 1% (w/v) Triton X-100, 0.2% (w/v) SDS (denaturing IPs). Proteins were eluted from the beads by heating at 95 °C in Laemmli buffer for 5 min and then separated by 14% SDS-PAGE. Gels were dried and imaged with Fuji FLA-3000 phosphorimaging.

Two-dimensional Gel Electrophoresis-BN-/SDS-PAGE—Inner membrane vesicles were prepared as described previously (23, 29) with few minor changes. Briefly, cells were grown in LB media by shaking at 37 °C to A_{600} = 0.9 then broken using an Emulsiflex-C3 (Avestin). Unbroken cells were pelleted by centrifugation for 10 min at 8000 × *g* at 4 °C. The membrane fraction was collected by ultracentrifugation for 60 min at 180,000 × *g* at 4 °C then separated into fractions containing inner and outer membrane vesicles using a six-step sucrose gradient. Inner membrane vesicles were resuspended in ACA_{750} buffer (750 mM *n*-amino-caproic acid, 50 mM Bis-Tris, 0.5 mM Na_2EDTA, pH 7.0), and the protein concentration was determined by the Bradford assay (Bio-Rad). Inner membrane proteins were solubilized by resuspending 500 μg of inner membrane vesicles in 100 μl of ACA_{750} buffer containing 1% (w/v) digitonin for 60 min on ice. Insoluble membrane debris was removed by centrifugation for 20 min at 264,000 × *g*, and the sample was mixed with 15 μl of G250 solution (5% (w/v) Coomassie G250 in ACA_{750} buffer). Samples were separated in the first dimension by 5–15% BN-PAGE and in the second dimension by 8–16% SDS-PAGE as described previously (23, 29). Proteins were blotted onto nitrocellulose membranes using a semi-dry blotting device (Bio-Rad) and decorated with rabbit antisera raised against YfgM/PpiD (see below), SecY, SecE, and YidC. A donkey anti-rabbit IgG horseradish peroxidase conjugate secondary antibody was used (GE Healthcare). For detection, the ECL system (GE Healthcare) and a LAS-1000 CCD camera (Fujifilm) were used. Images were analyzed with the Image Gauge Version 4.23 software (Fujifilm).

Production of YfgM/PpiD Antisera—The full-length YfgM and PpiD were co-purified as described in Maddalo *et al.* (23). A single rabbit polyclonal antisera was produced by Innovagen AB (Sweden).

Antibiotic Susceptibility Disc Assays—Cells were grown to an $A_{600\,nm} \approx 0.8$, and a volume equivalent to 0.2 A_{600} units was plated onto LB agar containing appropriate antibiotics (kanamycin 50 μg/ml and chloramphenicol 17 μg/ml). Cultures were evenly spread then let dry before discs containing 30 μg of vancomycin (Oxoid) were placed on the agar. Inhibition zone radii were measured after 16 h at 37 °C.

σE and Cpx Stress Response Assay—Reporter plasmids for σ^E- and Cpx-dependent envelope stress responses (*rpoE rseABC-gfp* and *ppiA-gfp*, respectively) were obtained from (30), and the kanamycin resistance cassette was replaced with a chloramphenicol resistance cassette. Strains were transformed with the plasmids and selected on LB agar supplemented with

[2] The abbreviations used are: IP, immunoprecipitation; BN, blue native; BAM, β-barrel assembly machine; Bis-Tris, 2-[bis(2-hydroxyethyl)amino]-2-(hydroxymethyl)propane-1,3-diol.

17 μg/ml chloramphenicol (and kanamycin if required by the host strain). Three colonies were grown in liquid LB media at 37 °C to an A_{600} of ~0.8. The cells were concentrated by centrifugation at 4000 × *g* and resuspended in 200 μl of buffer G (50 mM Tris-HCl, pH 8.0, 200 mM NaCl, 15 mM EDTA). Green fluorescent protein (GFP) fluorescence was measured (488-nm excitation − 512-nm emission) in a Spectramax GEMINI EM microplate reader (Molecular Devices) and normalized by the corresponding A_{600} value.

Purification of YfgM^{SOL} and PpiD^{SOL}—The regions encoding amino acids 45–206 of YfgM and 37–623 of PpiD were cloned downstream of a region coding for an octahistidine tag (−His_8) in the *pGFP$_E$* vector (a derivative of pET28a (31, 32)). The plasmids were individually transformed into the BL21(*DE3*) *pLysS* and grown in LB supplemented with 34 μg/ml chloramphenicol and 50 μg/ml kanamycin to an A_{600} of ~0.4. Protein expression was induced with 0.5 mM isopropyl 1-thio-β-D-galactopyranoside for 5 h at 37 °C. Cells were harvested by centrifugation at 8000 × *g* then resuspended in disruption buffer (PBS, pH 7.4, complete protease inhibitor (Roche Applied Science), 10 μg of DNAse I) and mechanically broken using an Emulsiflex-C3 (Avestin). Membrane debris was removed by ultracentrifugation at 180,000 × *g* for 1 h at 4 °C. The soluble fraction was supplemented with 10 mM imidazole and cycled over an equilibrated 5-ml HisTrap FF column (GE Healthcare). Impurities were removed with 10 column volumes of wash buffer (PBS, pH 7.4, 70 mM imidazole, 150 mM NaCl), and YfgM^{SOL}/PpiD^{SOL} were eluted by increasing the concentration of the wash buffer to 500 mM using a linear gradient of 100 ml. For further purification and buffer exchange to 20 mM Tris, pH 7.4, and 150 mM NaCl, a Superdex 200 10/300 column was used (GE Healthcare). Fractions containing the desired protein were pooled and concentrated using a 10-kDa cut-off concentrator (Sartorius Stedim A/S). SDS-PAGE analysis and Coomassie staining was used to assess the purity of the proteins.

Protein Aggregation Assays—Firefly luciferase aggregation was performed as described in Cajo *et al.* (33), except that luciferase was denatured for 90 min at 25 °C and aggregation kinetics were followed at 25 °C (34).

Unfolded proOmpC (200 μM in 20 mM Tris, pH 7.5, 200 mM NaCl, 1 mM DTT, 20% glycerol, 8 M urea) prewarmed for 10 min at 60 °C was diluted 100-fold in reaction buffer (30 mM Hepes, pH 7.5, 40 mM KCl, 50 mM NaCl, 7 mM magnesium acetate, and 1 mM DTT) preincubated at 25 °C with or without chaperones. Immediately after the addition of denatured proOmpC, aggregation was monitored continuously at 320 nm for 60 min at 25 °C on a Cary Scan UV-visible spectrophotometer from Varian. All solutions used in this assay were filtered through a 0.22-μm filter (35).

Malate dehydrogenase (1 μM monomer in the final reaction; Roche Applied Science) was incubated in the presence or absence of preincubated protein for 30 min at 30 °C or 47 °C in 50 μl of reaction buffer containing 50 mM Tris-HCl, pH 7.5, 150 mM KCl, 20 mM $MgCl_2$, 2 mM DTT. Samples were centrifuged for 30 min at 13,000 rpm at 4 °C. Supernatant and pellet were analyzed separately by 4–12% SDS-PAGE and then stained with Coomassie Blue.

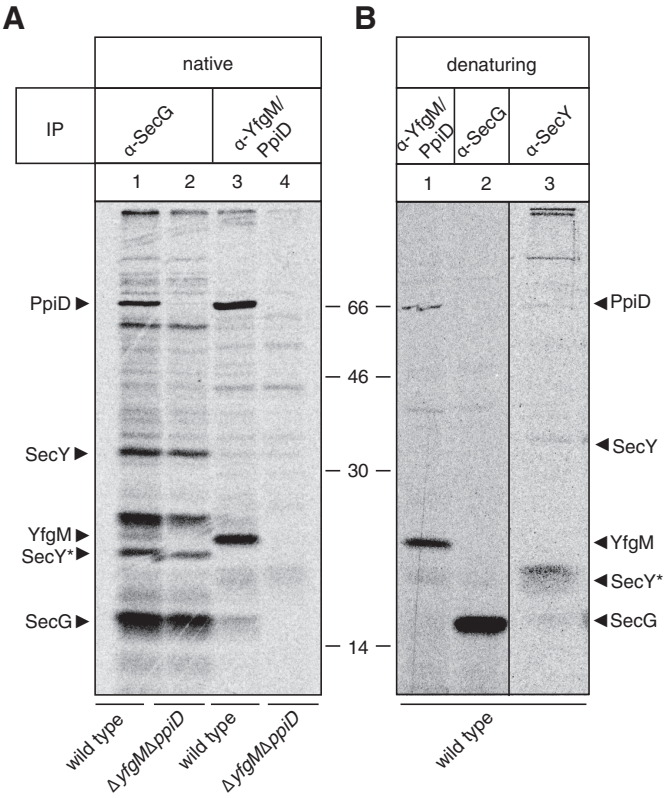

FIGURE 1. **YfgM and PpiD form a detergent-stable supercomplex with the Sec translocon.** *A*, IP of membrane protein complexes from wild type *E. coli* and the Δ*ppiD* Δ*yfgM* strain using antisera to SecG or YfgM/PpiD. Whole cells were pulse-labeled with [^{35}S]methionine and solubilized in buffer containing 1% (w/v) digitonin. The immunoprecipitation was carried out under native conditions so that interacting partners could be co-immunoprecipitated. *B*, IPs from wild type cells using antisera to SecY, SecG, and YfgM/PpiD were carried out under denaturing conditions to show the specificity of the antibodies and assign bands in *A*. Note that the lower molecular weight band observed for SecY indicated that it was the processed form (termed SecY*), as described by Akiyama and Ito (58).

RESULTS

YfgM Interacts with the SecYEG Translocon—To determine if YfgM interacts with the Sec translocon, we initially tried to detect it after co-IP with SecG antisera. We radiolabeled wild type cells with [^{35}S]methionine, extracted membrane protein complexes with digitonin and immunoprecipitated SecG using native conditions. Approximately 10 prominent bands were detected when the samples were analyzed by SDS-PAGE and autoradiography (Fig. 1*A*, *lane 1*). Two of the bands corresponded in molecular mass to YfgM (22 kDa) and PpiD (68 kDa) and could be assigned by repeating the experiment in a strain devoid of *yfgM* and *ppiD* (Fig. 1*A*, *lane 2*). Two bands appeared at the same molecular mass as SecY and the processed form of SecY, called SecY* (Fig. 1*A*, *lane 2 versus* Fig. 1*B*, *lane 3*). Other bands that were co-immunoprecipitated with the SecG antisera have not been assigned in this study, as this has been done previously (21).

We also performed a reciprocal co-IP. In this experiment SecG was co-immunoprecipitated with YfgM/PpiD antisera (Fig. 1*A*, *lane 3*). Notably, SecG was not co-immunoprecipitated in a strain devoid of *yfgM* and *ppiD* (Fig. 1*A*, *lane 4*); thus it is unlikely that the antisera unspecifically recognizes SecG. SecY was not detected in this experiment. We believe that this

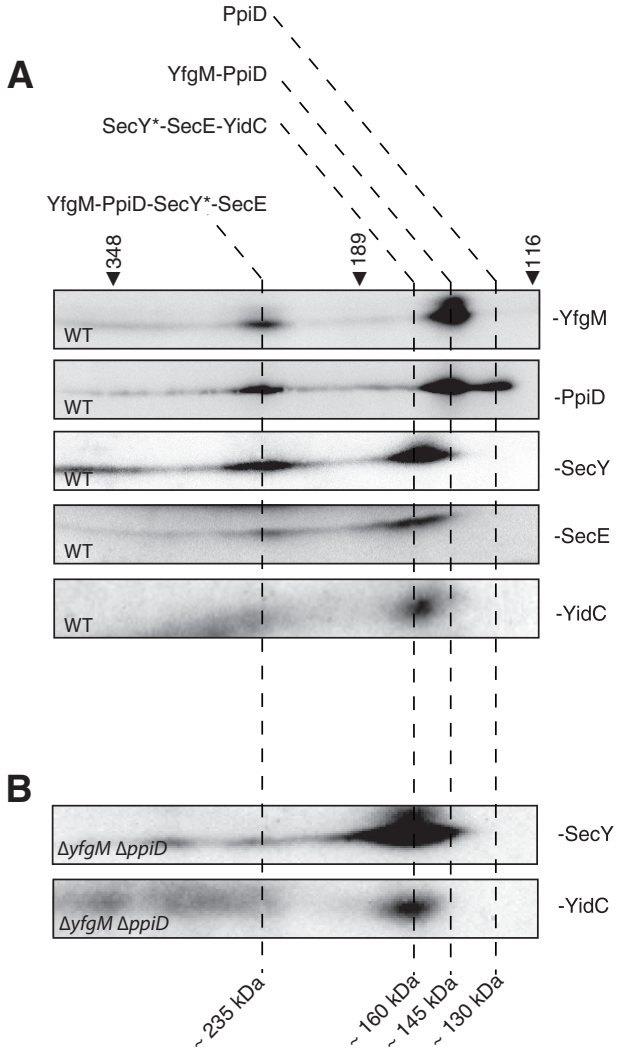

FIGURE 2. **Two-dimensional BN-/SDS-PAGE indicates that YfgM and PpiD are in complex with a sub-population of the Sec translocon.** *A*, inner membrane proteins from wild type *E. coli* were solubilized in 1% digitonin, separated by two-dimensional BN-/SDS-PAGE, blotted onto a nitrocellulose membrane, and immuno-decorated with protein-specific antisera. Proteins that align in vertical channels were deemed to be in complexes. Note that the molecular weight observed for SecY indicated that it was processed (termed SecY*), as described by Akiyama and Ito (58). *B*, SecY* shifts to a lower molecular mass when a Δ*ppiD* Δ*yfgM* strain is analyzed by two-dimensional BN-/SDS-PAGE. Molecular mass markers (in kDa) were calibrated to membrane proteins (29).

was a technical artifact rather than a biological observation, as we detected SecY when we co-immunoprecipitated with SecG antisera and in BN-PAGE analysis (see below).

To obtain complementary evidence that YfgM interacts with the translocon, we solubilized protein complexes from wild type inner membranes with digitonin then separated them by two-dimensional BN-/SDS-PAGE. Proteins were blotted onto a nitrocellulose membrane and identified with antisera raised against YfgM/PpiD, SecY, and SecE. All proteins aligned in a vertical channel of ~235 kDa, indicating that they had co-migrated in the non-denaturing BN-PAGE (Fig. 2*A*). The analysis also detected vertical channels containing YfgM and PpiD (~145 kDa) and PpiD only (~130 kDa) (Fig. 2*A*). Thus there appear to be populations of YfgM and PpiD that are independent from the translocon. Finally, we detected a complex containing SecY, SecE, and YidC (Fig. 2*A*). This latter observation suggests that there might be different populations of the Sec translocon.

Co-migration of proteins in BN-PAGE is usually considered proof that they form a detergent-stable complex. Nevertheless we substantiated our observation that YfgM and PpiD co-migrated with the Sec translocon by analyzing membrane protein complexes from the Δ*ppiD* Δ*yfgM* strain. In this experiment, the vast majority of SecY* shifted from ~235 to ~160 kDa (Fig. 2*B*). Taken together, the co-IP analyses and BN-PAGE unequivocally show that YfgM co-purifies with the SecYEG translocon when digitonin is used for solubilization of membrane proteins.

YfgM Contributes to Outer Membrane Integrity—Based on the fact that YfgM has a large periplasmic domain (23, 25) and that it associates with PpiD (see Ref. 23 and this study) we reasoned that it might play a role in the periplasmic network that includes SurA, Skp, DegP, PpiD, and FkpA (for review, see Refs. 10, 36, and 37). This network chaperones β-barrel proteins from the Sec translocon to the β-barrel assembly machine (BAM) in the outer membrane. SurA and Skp are the major players in the network, and strains lacking them are defective in their ability to traffic β-barrel proteins. As a result, the integrity of the outer membrane is compromised, and the cells are hypersensitive to antibiotics such as vancomycin and novobiocin (38–41). To determine if YfgM is also part of this network, we analyzed a Δ*yfgM* strain in an antibiotic susceptibility assay. The strain was obtained by replacing the open reading frame of *yfgM* with a kanamycin resistance gene. To exclude the possibility of a polar effect on the expression of *bamB* (which is also involved in outer membrane biogenesis and adjacent to *yfgM*), we verified that the levels of BamB remained constant by Western blotting (Fig. 3*A*). When we tested Δ*yfgM* in the antibiotic susceptibility disc assay, we did not observe a zone of growth inhibition around filter paper discs containing 30 μg of vancomycin (Fig. 3*B*). Thus we conclude that there is no obvious defect in the outer membrane of the Δ*yfgM* strain. Similar results were obtained for the Δ*degP* and Δ*ppiD* strains (Fig. 3*B*), which are considered to be minor players in this periplasmic chaperone network. In contrast, Δ*surA* and Δ*skp* show susceptibility to vancomycin, indicating that the outer membrane is compromised in these strains (Fig. 3*B*).

To determine if the lack of a phenotype in the Δ*yfgM* strain was caused by compensatory up-regulation of other periplasmic chaperones, we monitored the steady state levels of PpiD, Skp, and SurA by immunoblotting (Fig. 4). We detected a slight up-regulation of Skp, which might partly explain why the susceptibility to antibiotics was weak. A similar level of up-regulation of Skp was also observed in the Δ*ppiD* and Δ*surA* strains.

Because periplasmic chaperones often have overlapping functions, their involvement in a network can only be discerned by deleting them in combination. For example, the simultaneous deletion of *ppiD* and *degP* results in a temperature-sensitive phenotype (37), and deletion of *surA* and either *skp* or *degP* results in lethality (42). We engineered Δ*ppiD* Δ*yfgM*, Δ*degP* Δ*yfgM*, Δ*skp* Δ*yfgM*, and Δ*surA* Δ*yfgM* double deletions and again probed outer membrane integrity with vancomycin. All strains were obtained, indicating that the double deletions were

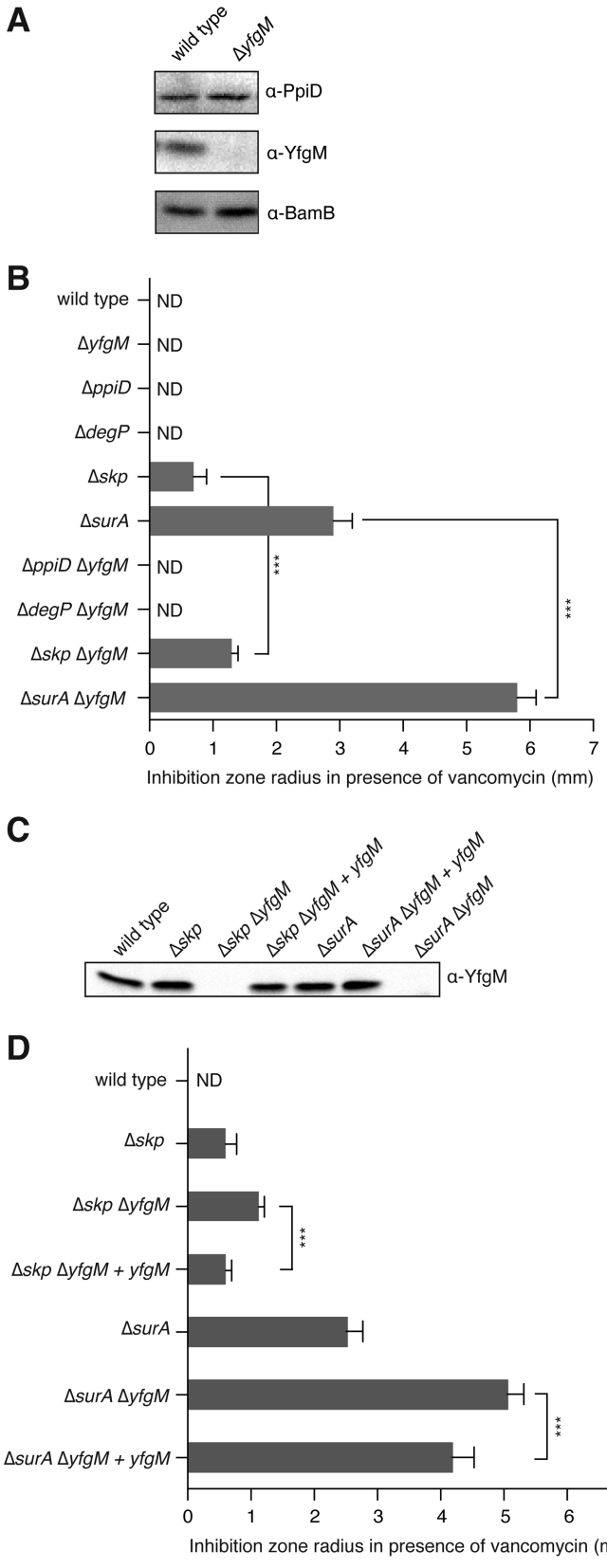

FIGURE 3. **Deletion of *yfgM* in combination with either *surA* or *skp* causes increased sensitivity to vancomycin.** *A*, Western blot showing that deletion of *yfgM* has no effect on the levels of BamB. *B*, the integrity of the outer membrane in wild type and deletion strains was assayed by measuring the inhibition zone radius (mm) when a filter disc containing 30 μg of vancomycin was placed on a lawn of cells. Each *bar* represents an average of at least three biological replica. *C*, immunoblot of wild type, deletion, and complemented strains illustrating the protein levels of YfgM. *D*, Δ*surA* Δ*yfgM* and Δ*skp* Δ*yfgM* strains were complemented using the pSC-*yfgM* plasmid, and the integrity of the outer membrane was assayed by measuring the inhibition zone radius (mm). Statistical significance was determined by an unpaired two-tailed Student's test assuming unequal variance. *Three stars* indicate a probability of $p < 0.001$. *ND*, not detected.

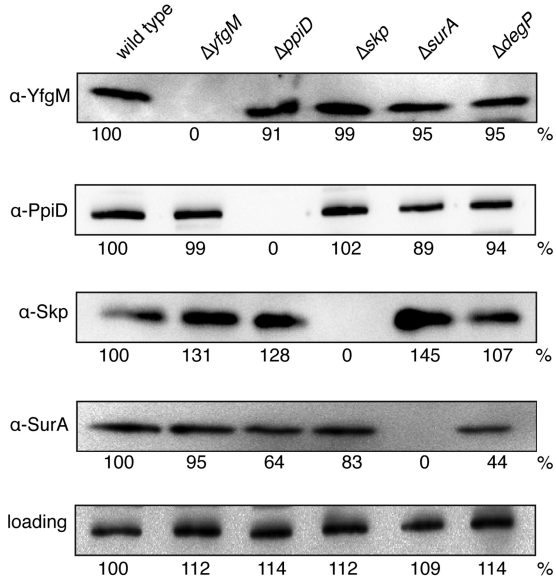

FIGURE 4. **Comparison of the steady state levels of periplasmic chaperones.** Wild type cells and single gene deletions were separated by 14% SDS-PAGE then immunoblotted. Signal intensities were quantified and normalized relative to the wild type protein.

viable. In the antibiotic susceptibility disc assays the Δ*ppiD* Δ*yfgM* and Δ*degP* Δ*yfgM* strains were insensitive to vancomycin, but the Δ*surA* Δ*yfgM* strain, and to a lesser extent the Δ*skp* Δ*yfgM* strain, were more sensitive to vancomycin than the respective single deletions (Fig. 3*B*). These same phenotypes were observed using novobiocin, indicating that they are not limited to the action of vancomycin (data not shown).

The vancomycin sensitivity of the Δ*skp* Δ*yfgM* double deletion could be reverted to that of the Δ*skp* single deletion by expressing *yfgM* from its native promoter in a low copy plasmid (Fig. 3, *C* and *D*). Plasmid expression of *yfgM* could partially revert the phenotype of the Δ*surA* Δ*yfgM* double deletion to that of the Δ*surA* mutant (Fig. 3, *C* and *D*). At this stage it is not clear why complementation was not completely effective in this strain. Taken together, the data indicate that deletion of *yfgM* further compromised the integrity of the outer membrane in both the Δ*surA* and Δ*skp* backgrounds. This observation suggests that the physiological role of YfgM overlaps to some degree with SurA and Skp.

Loss of YfgM Exacerbates the σ^E-Dependent Envelope Stress Response in a Δskp Deletion Strain—Deletion of periplasmic chaperones can result in an extracytoplasmic stress response. In *E. coli* there are two major systems for detecting extracytoplasmic stresses, the σ^E-dependent envelope stress response and the CpxAR two-component system (for review, see Refs. 43–46). Both systems trigger a signaling cascade that results in the up-regulation of envelope chaperones and/or proteases. We first tested for a σ^E-dependent envelope stress response using a plasmid containing the promoter region for the *rpoE*

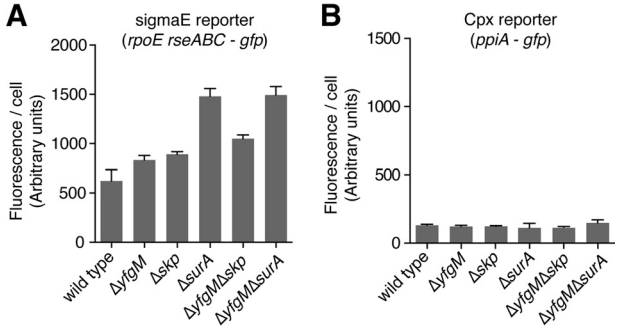

FIGURE 5. **Deletion of *yfgM* in combination with *skp* leads to increased envelope stress.** The transcription of *rpoE rseABC* (σ^E-dependent envelope stress response) (*A*) and *ppiA* (Cpx regulon) (*B*) were monitored using transcriptional fluorescence reporters (30) to evaluate envelope stress in deletion strains. All fluorescence data were normalized by the optical density at 600 nm and expressed as arbitrary fluorescence units per cell. Each data point represents the average of at least three biological replica.

rseABC operon adjacent to the gene encoding the GFP (30). Thus σ^E activity was inferred from whole cell fluorescence. In the Δ*yfgM* strain, the expression of GFP from the *rpoE rseABC* promoter was slightly higher than the wild type strain (Fig. 5*A*). The Δ*skp* Δ*yfgM* double deletion also resulted in a slightly stronger σ^E-dependent envelope stress response than the Δ*skp* deletion. Deletion of *yfgM* in the Δ*surA* background did not affect the strength of the σ^E response, which was already quite high in the Δ*surA* deletion strain (Fig. 5*A*).

We also tested for an envelope stress response through the CpxAR two-component system using a plasmid containing the promoter region for *ppiA* (a periplasmic peptidyl-prolyl *cis-trans*-isomerase). We did not detect elevated fluorescence levels in any of the deletion strains, indicating that the Cpx extracytoplasmic stress response was not activated by perturbations to the trafficking of β-barrel proteins (Fig. 5*B*). It is worth noting that others have detected a response in a *surA* deletion strain using a *cpxP-lacZ* reporter construct (37). We did not resolve this discrepancy, as it was not the main point of the study.

Our analyses of the outer membrane integrity and extracytoplasmic stress responses indicate that loss of *yfgM* exacerbates the phenotypes of both Δ*surA* and Δ*skp* strains. These observations strongly suggest a role for YfgM in the periplasmic chaperone network that traffics β-barrel proteins from the Sec translocon to the BAM.

PpiD Can Prevent Protein Aggregation but YfgM Cannot—How might YfgM assist β-barrel proteins as they exit from the Sec translocon? One obvious possibility is that YfgM delays aggregation of the polypeptide as it enters the periplasm, as shown for PpiD (37). To explore this possibility we carried out *in vitro* aggregation assays in the presence of a soluble version of YfgM ($YfgM^{SOL}$). For comparison, we also expressed and purified a soluble version of PpiD ($PpiD^{SOL}$). Both $YfgM^{SOL}$ and $PpiD^{SOL}$ showed mono-disperse profiles when analyzed by size-exclusion chromatography, indicating that the domains were folded (Fig. 6*A*). The size-exclusion chromatography traces also indicated that both domains formed homo-oligomeric species; however, we are not sure if these states are physiologically relevant. We then tested whether $YfgM^{SOL}$ + $PpiD^{SOL}$ could prevent aggregation of three test proteins, proOmpC, malate dehydrogenase, and luciferase. When the test proteins were denatured either chemically or by heat treatment and diluted into buffer, they aggregated (Fig. 6, *B–D*). For all three proteins, the aggregation could be inhibited by a molar excess of $PpiD^{SOL}$ but not of $YfgM^{SOL}$. Simultaneous addition of both $YfgM^{SOL}$ and $PpiD^{SOL}$ did not show a cooperative effect on aggregation of the test proteins; however, this was not surprising, as the two domains do not interact *in vitro* (Fig. 6*A*). Taken together, the data indicate that YfgM does not prevent protein aggregation; thus its role at the translocon may differ from that of PpiD.

DISCUSSION

Here we show that YfgM, an inner membrane protein with no annotated function, is an ancillary subunit of the Sec translocon. Initially we showed that YfgM and PpiD were physically associated with the translocon when solubilized with digitonin and analyzed by co-immunoprecipitation and two-dimensional BN-/SDS-PAGE. Both YfgM and PpiD contain a single transmembrane helix and a large periplasmic domain (23, 25, 26); thus it seems likely that the periplasmic domains reside in close proximity to the exit of the translocon. Curiously, our analysis also indicated that there was a population of YfgM-PpiD that was independent from SecYEG. It remains to be determined if this is a distinct population or whether YfgM-PpiD cycles on and off the translocon.

The Sec translocon interacts with a number of ancillary modules, such as SecA, SecDF-YajC, and YidC (19, 47–51), and it is not clear if they are present simultaneously. Unfortunately we were unable to determine whether SecA and SecDF-YajC were associated with the translocon at the same time as YfgM-PpiD, as antisera were not available. We were able to confirm that YidC associated with the translocon, but notably, it was not detected on those translocons that were associated with YfgM-PpiD. This may be because digitonin does not solubilize all supercomplexes or that the Sec translocon cannot associate with YfgM-PpiD and YidC simultaneously.

The Sec translocon has been extensively studied in *E. coli*, so why hasn't YfgM been previously detected as an ancillary module? Most other studies (including our own) have solubilized proteins with detergents such as n-dodecyl-B-D-maltoside (DDM) or β-octyl glucoside and have not detected the association (21–23). Thus we reason that it is only possible to co-purify YfgM with the Sec translocon if digitonin is used as a detergent, as we have done here. This observation is consistent with a large body of work that has shown that respiratory supercomplexes are sensitive to all detergents except digitonin (52).

What role does YfgM play at the translocon? Because YfgM physically interacts with PpiD (23), we reasoned that it might have a similar function. PpiD facilitates the release of β-barrel proteins into the periplasm (24) by preventing premature aggregation (37). The β-barrel proteins are then chaperoned across the periplasmic space by SurA, Skp, and DegP and delivered to the BAM complex in the outer membrane (10, 36, 37). Evidence that YfgM is involved in this network was primarily obtained by monitoring outer membrane integrity in strains lacking *yfgM*. We noted that strains lacking *surA* and *skp* became more sensitive to vancomycin and novobiocin when

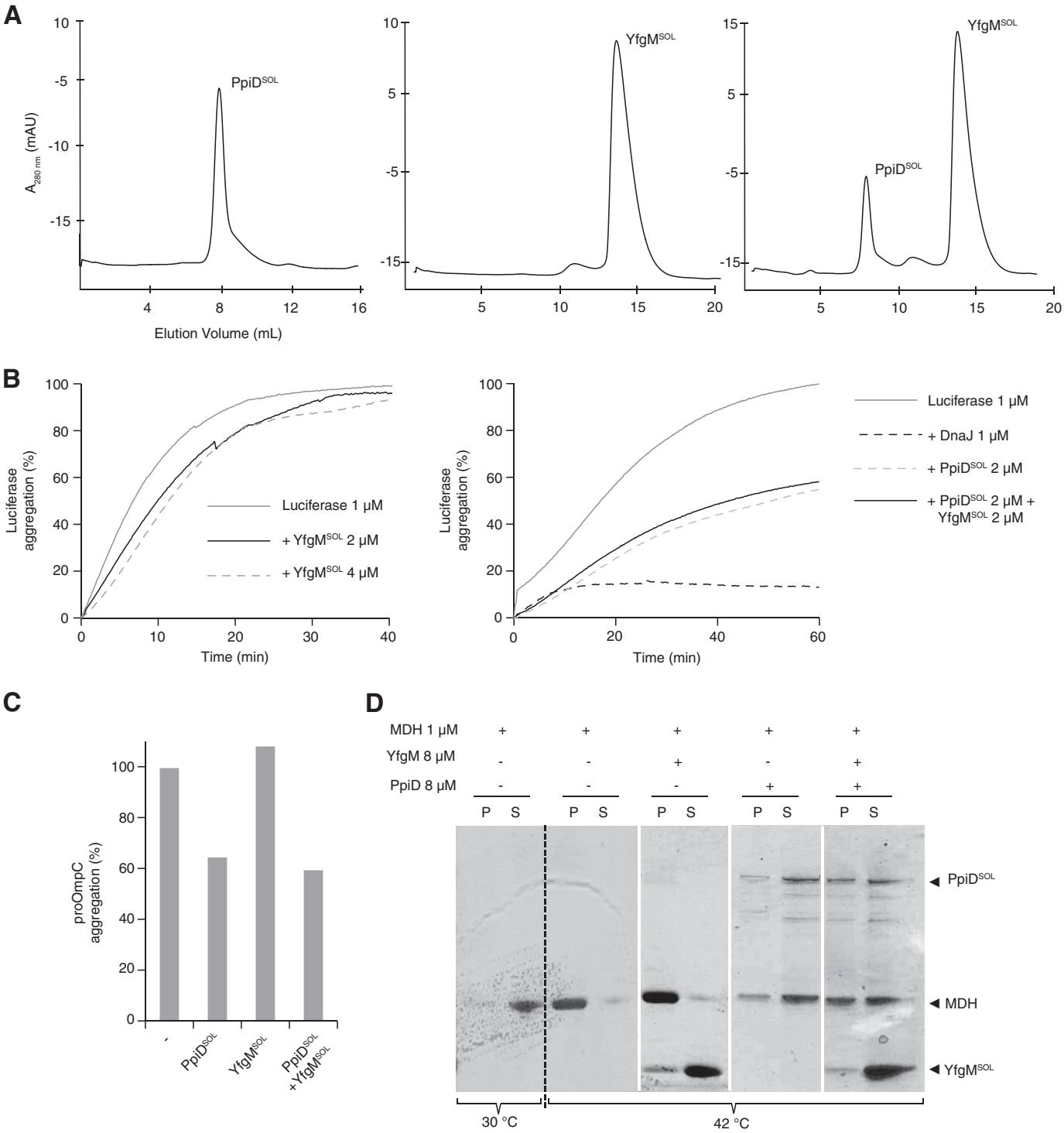

FIGURE 6. **YfgM^{SOL} cannot prevent protein aggregation activity *in vitro* but PpiD^{SOL} can.** *A*, purified PpiD^{SOL}, YfgM^{SOL}, or both were analyzed by size exclusion chromatography. *mAU*, milliabsorbance units. *B*, luciferase aggregation protection assay. Optical densities were measured at 320 nm, and the percentage values were normalized to the luciferase aggregation obtained in the absence of added chaperones. *Left panel*, a representative plot of a luciferase aggregation protection assay is shown with chemically denatured luciferase 1 μM alone (*gray line*) or in the presence of YfgM^{SOL} 2 μM (*black line*) or 4 μM (*gray dashed line*). *Right panel*, a representative plot of a luciferase aggregation protection assay is shown with chemically denatured luciferase 1 μM alone (*gray line*) or in the presence of DnaJ 1 μM (*black dashed line*), PpiD^{SOL} 2 μM (*gray dashed line*) or both PpiD^{SOL} 2 μM and YfgM^{SOL} 2 μM (*black line*). *C*, aggregation of denatured proOmpC (2 μM) at 25 °C after a 50-min reaction in the presence of 8 μM PpiD^{SOL}, 8 μM YfgM^{SOL}, and both 8 μM PpiD^{SOL} and 16 μM YfgM^{SOL} or in the absence of chaperone (−). The percentage of aggregation was normalized to proOmpC aggregation obtained when no chaperone was added. *D*, malate dehydrogenase (*MDH*) aggregation protection assay. Interaction of native malate dehydrogenase (with PpiD^{SOL}, YfgM^{SOL}, or both as indicated above the gel. Samples were incubated at 42 °C and centrifuged to analyze the resulting supernatant (*S*) and pellets (*P*) containing malate dehydrogenase and associated proteins aggregates by SDS-PAGE and stained with Coomassie Blue.

yfgM was deleted. Thus, indicating that the integrity of the outer membrane was further compromised in the absence of YfgM. Notably we also detected an exacerbated σ^E extracytoplasmic stress response when *yfgM* was deleted in a Δ*skp* background. We did not detect an exacerbated σ^E extracytoplasmic stress response when *yfgM* was deleted in the Δ*surA* background. This observation was surprising as the phenotype of the Δ*surA* Δ*yfgM* strain was more pronounced than the Δ*surA* strain in the antibiotic sensitivity assays. A possible explanation might be that the σ^E-dependent extracytoplasmic stress response was already fully activated in the Δ*surA* strain. Taken together, the simplest interpretation of these data is that the physiological role of YfgM overlaps with SurA and Skp. This role is different to that of PpiD as we noted differences between YfgM and PpiD during our characterization.

Further work is required to understand the molecular role of YfgM at the Sec translocon. One possibility is that it acts as a docking point for SurA and Skp. Both of these proteins engage substrate proteins near the translocon (53); however, the molecular details of this engagement are vague. An interesting precedence for the involvement of a docking protein at the Sec translocon can be found in the endoplasmic reticulum of *Arabidopsis thaliana* (54), where *At*TPR7 mediates docking of Hsp70/90. Although *At*TPR7 is unrelated to YfgM, both proteins contain tetratrico-peptide repeat (TPR) domains (for review, see Ref. 55), which are often involved in protein-protein interactions. Another possible role for YfgM may be in the acid stress response, as *E. coli* cells are more susceptible to acid stress when YfgM is overexpressed (56). The acid stress response involves a number of periplasmic chaperones that refold SurA, DegP, FkpA, and PpiD after acid damage (57). All of these potential roles warrant further exploration, as they will provide a better understanding of YfgM and its role in protein secretion through the Sec translocon.

Acknowledgments—We are grateful to Marcelo Sousa, Tom Silhavy, and Jan Willem de Gier for strains and antisera.

REFERENCES

1. Dalbey, R. E., and Kuhn, A. (2012) Protein traffic in Gram-negative bacteria: how exported and secreted proteins find their way. *FEMS Microbiol. Rev.* **36,** 1023–1045
2. Economou, A. (2000) Bacterial protein translocase: a unique molecular machine with an army of substrates. *FEBS Lett.* **476,** 18–21
3. Park, E., and Rapoport, T. A. (2012) Mechanisms of Sec61/SecY-mediated protein translocation across membranes. *Annu. Rev. Biophys.* **41,** 21–40
4. Rapoport, T. A. (2007) Protein translocation across the eukaryotic endoplasmic reticulum and bacterial plasma membranes. *Nature* **450,** 663–669
5. du Plessis, D. J., Nouwen, N., and Driessen, A. J. (2011) The Sec translocase. *Biochim. Biophys. Acta* **1808,** 851–865
6. Lycklama A Nijeholt, J. A., and Driessen, A. J. (2012) The bacterial Sec-translocase: structure and mechanism. *Philos. Trans. R Soc. Lond. B Biol. Sci.* **367,** 1016–1028
7. Dautin, N., and Bernstein, H. D. (2007) Protein secretion in gram-negative bacteria via the autotransporter pathway. *Annu. Rev. Microbiol.* **61,** 89–112
8. Leyton, D. L., Rossiter, A. E., and Henderson, I. R. (2012) From self-sufficiency to dependence: mechanisms and factors important for autotransporter biogenesis. *Nat. Rev. Microbiol.* **10,** 213–225
9. Okuda, S., and Tokuda, H. (2011) Lipoprotein sorting in bacteria. *Annu. Rev. Microbiol.* **65,** 239–259
10. Rigel, N. W., and Silhavy, T. J. (2012) Making a β-barrel: assembly of outer membrane proteins in Gram-negative bacteria. *Curr. Opin. Microbiol.* **15,** 189–193
11. Ruiz, N., Kahne, D., and Silhavy, T. J. (2006) Advances in understanding bacterial outer-membrane biogenesis. *Nat. Rev. Microbiol.* **4,** 57–66
12. Egea, P. F., and Stroud, R. M. (2010) Lateral opening of a translocon upon entry of protein suggests the mechanism of insertion into membranes. *Proc. Natl. Acad. Sci. U.S.A.* **107,** 17182–17187
13. Tsukazaki, T., Mori, H., Fukai, S., Ishitani, R., Mori, T., Dohmae, N., Perederina, A., Sugita, Y., Vassylyev, D. G., Ito, K., and Nureki, O. (2008) Conformational transition of Sec machinery inferred from bacterial SecYE structures. *Nature* **455,** 988–991
14. Van den Berg, B., Clemons, W. M., Jr., Collinson, I., Modis, Y., Hartmann, E., Harrison, S. C., and Rapoport, T. A. (2004) X-ray structure of a protein-conducting channel. *Nature* **427,** 36–44
15. Zimmer, J., Nam, Y., and Rapoport, T. A. (2008) Structure of a complex of the ATPase SecA and the protein-translocation channel. *Nature* **455,** 936–943
16. Samuelson, J. C., Chen, M., Jiang, F., Möller, I., Wiedmann, M., Kuhn, A., Phillips, G. J., and Dalbey, R. E. (2000) YidC mediates membrane protein insertion in bacteria. *Nature* **406,** 637–641
17. Scotti, P. A., Urbanus, M. L., Brunner, J., de Gier, J. W., von Heijne, G., van der Does, C., Driessen, A. J., Oudega, B., and Luirink, J. (2000) YidC, the *Escherichia coli* homologue of mitochondrial Oxa1p, is a component of the Sec translocase. *EMBO J.* **19,** 542–549
18. Sachelaru, I., Petriman, N. A., Kudva, R., Kuhn, P., Welte, T., Knapp, B., Drepper, F., Warscheid, B., and Koch, H. G. (2013) YidC occupies the lateral gate of the SecYEG translocon and is sequentially displaced by a nascent membrane protein. *J. Biol. Chem.* **288,** 16295–16307
19. Duong, F., and Wickner, W. (1997) The SecDFyajC domain of preprotein translocase controls preprotein movement by regulating SecA membrane cycling. *EMBO J.* **16,** 4871–4879
20. Tsukazaki, T., Mori, H., Echizen, Y., Ishitani, R., Fukai, S., Tanaka, T., Perederina, A., Vassylyev, D. G., Kohno, T., Maturana, A. D., Ito, K., and Nureki, O. (2011) Structure and function of a membrane component SecDF that enhances protein export. *Nature* **474,** 235–238
21. Duong, F., and Wickner, W. (1997) Distinct catalytic roles of the SecYE, SecG, and SecDFyajC subunits of preprotein translocase holoenzyme. *EMBO J.* **16,** 2756–2768
22. Boy, D., and Koch, H. G. (2009) Visualization of distinct entities of the SecYEG translocon during translocation and integration of bacterial proteins. *Mol. Biol. Cell* **20,** 1804–1815
23. Maddalo, G., Stenberg-Bruzell, F., Götzke, H., Toddo, S., Björkholm, P., Eriksson, H., Chovanec, P., Genevaux, P., Lehtiö, J., Ilag, L. L., and Daley, D. O. (2011) Systematic analysis of native membrane protein complexes in *Escherichia coli*. *J. Proteome Res.* **10,** 1848–1859
24. Antonoaea, R., Fürst, M., Nishiyama, K., and Müller, M. (2008) The periplasmic chaperone PpiD interacts with secretory proteins exiting from the SecYEG translocon. *Biochemistry* **47,** 5649–5656
25. Toddo, S., Söderström, B., Palombo, I., von Heijne, G., Nørholm, M. H., and Daley, D. O. (2012) Application of split-green fluorescent protein for topology mapping membrane proteins in *Escherichia coli*. *Protein Sci.* **21,** 1571–1576
26. Dartigalongue, C., and Raina, S. (1998) A new heat-shock gene, ppiD, encodes a peptidyl-prolyl isomerase required for folding of outer membrane proteins in *Escherichia coli*. *EMBO J.* **17,** 3968–3980
27. Baba, T., Ara, T., Hasegawa, M., Takai, Y., Okumura, Y., Baba, M., Datsenko, K. A., Tomita, M., Wanner, B. L., and Mori, H. (2006) Construction of *Escherichia coli* K-12 in-frame, single-gene knockout mutants: the Keio collection. *Mol. Syst. Biol.* **2,** 2006.0008
28. Datsenko, K. A., and Wanner, B. L. (2000) One-step inactivation of chromosomal genes in *Escherichia coli* K-12 using PCR products. *Proc. Natl. Acad. Sci. U.S.A.* **97,** 6640–6645
29. Stenberg, F., Chovanec, P., Maslen, S. L., Robinson, C. V., Ilag, L. L., von Heijne, G., and Daley, D. O. (2005) Protein complexes of the *Escherichia coli* cell envelope. *J. Biol. Chem.* **280,** 34409–34419

30. Zaslaver, A., Bren, A., Ronen, M., Itzkovitz, S., Kikoin, I., Shavit, S., Liebermeister, W., Surette, M. G., and Alon, U. (2006) A comprehensive library of fluorescent transcriptional reporters for *Escherichia coli*. *Nat. Methods* **3,** 623–628
31. Daley, D. O., Rapp, M., Granseth, E., Melén, K., Drew, D., and von Heijne, G. (2005) Global topology analysis of the *Escherichia coli* inner membrane proteome. *Science* **308,** 1321–1323
32. Rapp, M., Drew, D., Daley, D. O., Nilsson, J., Carvalho, T., Melén, K., De Gier, J. W., and Von Heijne, G. (2004) Experimentally based topology models for *E. coli* inner membrane proteins. *Protein Sci.* **13,** 937–945
33. Cajo, G. C., Horne, B. E., Kelley, W. L., Schwager, F., Georgopoulos, C., and Genevaux, P. (2006) The role of the DIF motif of the DnaJ (Hsp40) co-chaperone in the regulation of the DnaK (Hsp70) chaperone cycle. *J. Biol. Chem.* **281,** 12436–12444
34. Perrody, E., Cirinesi, A. M., Desplats, C., Keppel, F., Schwager, F., Tranier, S., Georgopoulos, C., and Genevaux, P. (2012) bacteriophage-encoded J-domain protein interacts with the DnaK/Hsp70 chaperone and stabilizes the heat-shock factor δ32 of *Escherichia coli*. *PLoS Genet.* **8,** e1003037
35. Bordes, P., Cirinesi, A. M., Ummels, R., Sala, A., Sakr, S., Bitter, W., and Genevaux, P. (2011) SecB-like chaperone controls a toxin-antitoxin stress-responsive system in *Mycobacterium tuberculosis*. *Proc. Natl. Acad. Sci. U.S.A.* **108,** 8438–8443
36. Ricci, D. P., and Silhavy, T. J. (2012) The Bam machine: a molecular cooper. *Biochim. Biophys. Acta* **1818,** 1067–1084
37. Matern, Y., Barion, B., and Behrens-Kneip, S. (2010) PpiD is a player in the network of periplasmic chaperones in *Escherichia coli*. *BMC Microbiol.* **10,** 251
38. Liu, A., Tran, L., Becket, E., Lee, K., Chinn, L., Park, E., Tran, K., and Miller, J. H. (2010) Antibiotic sensitivity profiles determined with an *Escherichia coli* gene knockout collection: generating an antibiotic bar code. *Antimicrob. Agents Chemother.* **54,** 1393–1403
39. Lazar, S. W., and Kolter, R. (1996) SurA assists the folding of *Escherichia coli* outer membrane proteins. *J. Bacteriol.* **178,** 1770–1773
40. Rouvière, P. E., and Gross, C. A. (1996) SurA, a periplasmic protein with peptidyl-prolyl isomerase activity, participates in the assembly of outer membrane porins. *Genes Dev.* **10,** 3170–3182
41. Schwalm, J., Mahoney, T. F., Soltes, G. R., and Silhavy, T. J. (2013) Role for Skp in LptD Assembly in *Escherichia coli*. *J. Bacteriol.* **195,** 3734–3742
42. Rizzitello, A. E., Harper, J. R., and Silhavy, T. J. (2001) Genetic evidence for parallel pathways of chaperone activity in the periplasm of *Escherichia coli*. *J. Bacteriol.* **183,** 6794–6800
43. Alba, B. M., and Gross, C. A. (2004) Regulation of the *Escherichia coli* δ-dependent envelope stress response. *Mol. Microbiol.* **52,** 613–619
44. Raivio, T. L., and Silhavy, T. J. (2001) Periplasmic stress and ECF δ factors. *Annu. Rev Microbiol.* **55,** 591–624
45. Ruiz, N., and Silhavy, T. J. (2005) Sensing external stress: watchdogs of the *Escherichia coli* cell envelope. *Curr. Opin. Microbiol.* **8,** 122–126
46. Rowley, G., Spector, M., Kormanec, J., and Roberts, M. (2006) Pushing the envelope: extracytoplasmic stress responses in bacterial pathogens. *Nat. Rev. Microbiol.* **4,** 383–394
47. Gardel, C., Benson, S., Hunt, J., Michaelis, S., and Beckwith, J. (1987) secD, a new gene involved in protein export in *Escherichia coli*. *J. Bacteriol.* **169,** 1286–1290
48. Gardel, C., Johnson, K., Jacq, A., and Beckwith, J. (1990) The secD locus of *E. coli* codes for two membrane proteins required for protein export. *EMBO J.* **9,** 4205–4206
49. Fang, J., and Wei, Y. (2011) Expression, purification and characterization of the *Escherichia coli* integral membrane protein YajC. *Protein Pept. Lett.* **18,** 601–608
50. Nouwen, N., and Driessen, A. J. (2002) SecDFyajC forms a heterotetrameric complex with YidC. *Mol. Microbiol.* **44,** 1397–1405
51. Kato, Y., Nishiyama, K., and Tokuda, H. (2003) Depletion of SecDF-YajC causes a decrease in the level of SecG: implication for their functional interaction. *FEBS Lett.* **550,** 114–118
52. Schägger, H. (2002) Respiratory chain supercomplexes of mitochondria and bacteria. *Biochim. Biophys. Acta* **1555,** 154–159
53. Ieva, R., Tian, P., Peterson, J. H., and Bernstein, H. D. (2011) Sequential and spatially restricted interactions of assembly factors with an autotransporter β domain. *Proc. Natl. Acad. Sci. U.S.A.* **108,** E383–E391
54. Schweiger, R., Müller, N. C., Schmitt, M. J., Soll, J., and Schwenkert, S. (2012) AtTPR7 is a chaperone-docking protein of the Sec translocon in *Arabidopsis*. *J. Cell Sci.* **125,** 5196–5207
55. Cerveny, L., Straskova, A., Dankova, V., Hartlova, A., Ceckova, M., Staud, F., and Stulik, J. (2013) Tetratricopeptide repeat motifs in the world of bacterial pathogens: role in virulence mechanisms. *Infect. Immun.* **81,** 629–635
56. Westphal, K., Langklotz, S., Thomanek, N., and Narberhaus, F. (2012) A trapping approach reveals novel substrates and physiological functions of the essential protease FtsH in *Escherichia coli*. *J. Biol. Chem.* **287,** 42962–42971
57. Zhang, M., Lin, S., Song, X., Liu, J., Fu, Y., Ge, X., Fu, X., Chang, Z., and Chen, P. R. (2011) A genetically incorporated crosslinker reveals chaperone cooperation in acid resistance. *Nat. Chem. Biol.* **7,** 671–677
58. Akiyama, Y., and Ito, K. (1990) SecY protein, a membrane-embedded secretion factor of *E. coli*, is cleaved by the ompT protease *in vitro*. *Biochem. Biophys. Res. Commun.* **167,** 711–715